Available online at www.sciencedirect.com
ScienceDirect
Journal of Colloid and Interface Science 310 (2007) 90–98
JOURNAL OF Colloid and Interface Science
www.elsevier.com/locate/jcis

Corrosion inhibition and adsorption behavior of methionine on mild steel in sulfuric acid and synergistic effect of iodide ion

E.E. Oguzie [a,b,*], Y. Li [a], F.H. Wang [a]

[a] *State Key Laboratory for Corrosion and Protection, Institute of Metal Research, Chinese Academy of Sciences, 62 Wencui Road Shenyang 110016, China*
[b] *Electrochemistry and Materials Science Research Laboratory, Department of Chemistry, Federal University of Technology Owerri, PMB 1526, Owerri, Nigeria*

Received 24 November 2006; accepted 17 January 2007
Available online 28 February 2007

Abstract

The corrosion inhibition of mild steel in sulfuric acid by methionine (MTI) was investigated using electrochemical techniques. The effect of KI additives on corrosion inhibition efficiency was also studied. The results reveal that MTI inhibited the corrosion reaction by adsorption onto the metal/solution interface. Inhibition efficiency increased with MTI concentration and synergistically increased in the presence of KI, with an optimum [KI]/[MTI] ratio of 5/5, due to stabilization of adsorbed MTI cations as revealed by AFM surface morphological images. Potentiodynamic polarization data suggest that the compound functioned via a mixed-inhibition mechanism. This observation was further corroborated by the fit of the experimental adsorption data to the Temkin and Langmuir isotherms. The inhibition mechanism has been discussed vis-à-vis the presence of both nitrogen and sulfur atoms in the MTI molecule.

Keywords: Mild steel; Corrosion inhibition; Adsorption; Amino acid; Iodide ion; Synergism

1. Introduction

Excessive corrosion attack is known to occur on mild steel surfaces deployed in service in aqueous acidic environments. In efforts to mitigate electrochemical corrosion, the primary strategy is to isolate the metal from corrosive agents. A useful method for achieving in this is addition of species to the solution in contact with the surface in order to inhibit the corrosion reaction and reduce the corrosion rate. Owing to increasing ecological awareness and strict environmental regulations and the need to develop environmentally friendly processes, attention is now focused on the development of substitute nontoxic alternatives to inorganic inhibitors applied earlier. Natural products extracted from plant sources [1–5], as well as some nontoxic organic compounds, which contain polar functions with nitrogen, oxygen, and/or sulfur in conjugated systems in their molecules [6–12], have been effectively used as inhibitors in many corrosion systems. The inhibiting action of such compounds is attributed as a first stage to the adsorption of the additives to the metal/solution interface. Inhibitor adsorption on mild steel in acid solutions usually leads to a structural modification in the double layer with subsequent reduction in the rates of the electrochemical half-cell reactions—the anodic metal dissolution and the cathodic reduction of hydrogen ions. To further upgrade the performance of organic inhibitors, extensive studies have been undertaken to identify synergistic effects of other additives. Interestingly, addition of halide ions to sulfuric acid solutions containing some organic compound has been reported to yield the required enhancement [9–14].

The roles of the individual functional groups in the inhibition mechanism of organic molecules have been widely reported, but the effect of having two different groups in one molecule, which may influence the corrosion process by different mechanisms, has not been properly documented and is an important consideration in this study. The test inhibitor for the present study is methionine [CH_3–S–CH_2–CH_2–$CH(CO_2H)NH_2$], an amino acid containing both the (–NH_2) and (–S–CH_3) groups in its molecule. Amino acids are attractive as corrosion inhibitors because they are relatively easy to produce with high purity at

* Corresponding author.
E-mail address: oguziemeka@yahoo.com (E.E. Oguzie).

0021-9797/$ – see front matter
doi:10.1016/j.jcis.2007.01.038

low cost and are soluble in aqueous media. Ashassi-Sorkhabi et al. [15] reported the successful application of methionine as a corrosion inhibitor for aluminum in mixed acid solution and pointed out the role of the S atom in increasing the interaction of the molecule with the metal surface. Morad et al. [5], in their study of the inhibiting effect of methionine on mild steel corrosion in phosphoric acid, observed that adsorption of the compound onto the metal surface obeyed the Frumkin isotherm with an adsorption free energy (ΔG^0_{ads}) value of 25.4 kJ mol^{-1}.

The present study investigates the inhibition mechanism of methionine on mild steel corrosion in sulfuric acid solution using electrochemical techniques. In addition to providing information on the corrosion rate, electrochemical techniques are well suited for monitoring in situ any perturbation by an inhibitor with respect to electrochemical processes in the metal/corrodent interface. The influence of iodide ions on the adsorption and corrosion-inhibitive properties of methionine has also been studied in order to ascertain the specific mode (ionic or molecular) in which the compound exerts its inhibiting action. Morphological changes on the corroding steel surface have been visualized by atomic force microscopy (AFM).

2. Experimental

Tests were performed on a mild steel specimen of the percentage composition C: 0.22; Si: 0.1–0.3; Mn: 0.6; P: 0.045. This was machined into test electrodes of dimension 1 × 1 cm and fixed in polytetrafluoroethylene (PTFE) rods by epoxy resin in such a way that only one surface, of area 1 cm^2, was left uncovered. The exposed surface was wet-polished with silicon carbide abrasive paper (from grade #200 to #1000), degreased in acetone, rinsed with distilled water, and dried in warm air. The aggressive solution was 0.5 M H_2SO_4 solution, prepared from analytical reagent grade sulfuric acid and distilled water. The test inhibitor methionine (MTI), obtained from (SCRC, China), was dissolved in 0.5 M H_2SO_4 solution to obtain the desired concentration (0.05–10 mM). Potassium iodide solutions (0.5–5.0 mM) were prepared in the blank corrodent and in 5.0 mM MTI.

Electrochemical experiments were conducted in a conventional three-electrode glass cell of capacity 400 ml, using a PARC Parstat-2273 Advanced Electrochemical System. A platinum foil was used as counterelectrode and a saturated calomel electrode (SCE) as reference electrode. The latter was connected via a Luggin's capillary. Electrochemical impedance spectroscopy (EIS) tests were performed at the end of 30 min of immersion at 30 ± 1 °C. Measurements were made at corrosion potentials (E_{corr}) over a frequency range of 100 kHz–10 MHz, with a signal amplitude perturbation of 5 mV. The data were collected using Powersine software and interpreted with Zsimpwin software, also supplied by PARC. Polarization studies were carried out after the EIS tests with Powercorr software in the potential range ±250 mV versus corrosion potential (E_{corr}) at a scan rate of 0.333 mV s^{-1}. The linear Tafel segments of the anodic and cathodic curves were extrapolated to corrosion potential to obtain the corrosion current densities (i_{corr}). Each test was run in triplicate to verify the reproducibility and the average values reported.

Morphological studies of the mild steel electrode surface were undertaken by atomic force microscopy, AFM (PicoPlus scanning probe microscope, Molecular Imaging Corp.). AFM images were realized in tapping mode at room temperature. Mild steel specimens of dimensions 15 × 10 × 2 mm were cleaned as previously described and immersed for 3 h in the blank solution (0.5 M H_2SO_4) and in 5.0 mM MTI and 5.0 mM MTI + 5.0 mM KI solutions at 30 ± 2 °C, and then washed with distilled water, dried in warm air, and submitted for AFM surface examination.

3. Results and discussion

3.1. Corrosion inhibition by methionine (MTI)

Measurements were undertaken to assess the impedance parameters of the mild steel/electrolyte interface in the presence of different concentrations of MTI. Representative examples of the impedance spectra are given in Fig. 1, panels a, b, and c, which exemplify, respectively, the Nyquist, Bode, and phase-angle plots obtained for mild steel in 0.5 M H_2SO_4 solution in the absence and presence of 0.05–10 mM MTI. The spectra obtained without and with inhibitor consist of one depressed capacitive loop corresponding to one time constant in the Bode plots. The high-frequency part of the impedance and phase angle describes the behavior of an inhomogeneous surface layer, whereas the low-frequency component depicts the kinetic response for the charge transfer reaction [16]. It is observed that increasing the concentration of MTI results in an increase in the size of the semicircle in Fig. 1a, in the impedance of the interface in Fig. 1b, and in the maximum phase angle in Fig. 1c, which indicate inhibition of the corrosion process. The impedance spectra for the Nyquist plots were analyzed by fitting to the equivalent circuit model shown in Fig. 2, which has been used previously to model the mild steel/acid interface [17,18]. The circuit comprises a solution resistance R_s shorted by a constant phase element (CPE) that is placed in parallel to the charge transfer resistance R_{ct}. The value of the charge transfer resistance is indicative of electron transfer across the interface. The use of the CPE, defined by the values Q and n, has been extensively described in the literature [19,20] and is employed in the model to compensate for the inhomogeneities in the electrode surface as depicted by the depressed nature of the Nyquist semicircle. The introduction of such a CPE is often used to interpret data for rough solid electrodes. The impedance, Z, of the CPE is [19,20]

$$Z_{CPE} = Q^{-1}(j\omega)^{-n}, \tag{1}$$

where Q and n stand for the CPE constant and exponent, respectively, $j = (-1)^{1/2}$ is an imaginary number, and ω is the angular frequency in rad s^{-1} ($\omega = 2\pi f$ when f is the frequency in Hz). The values of the double-layer capacitance, C_{dl}, were obtained at the frequency at which the imaginary component of

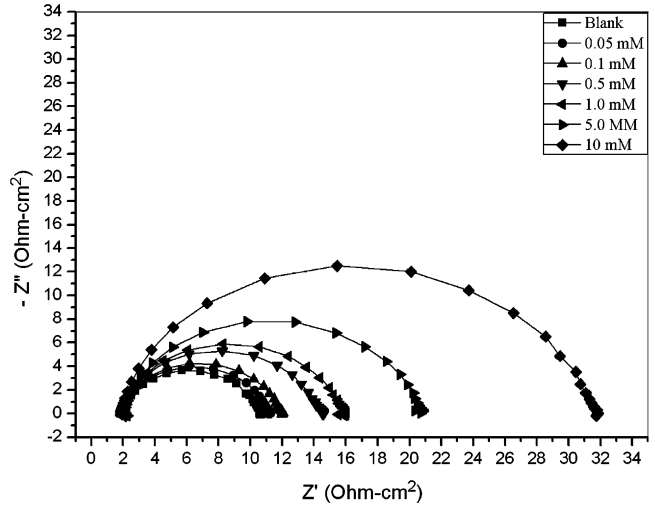

(a)

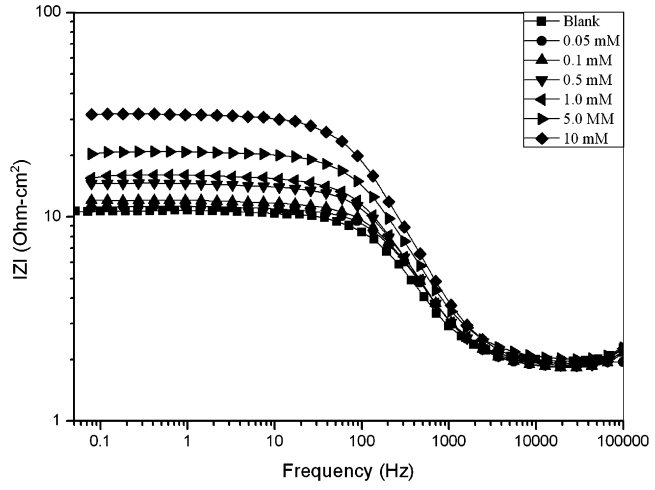

(b)

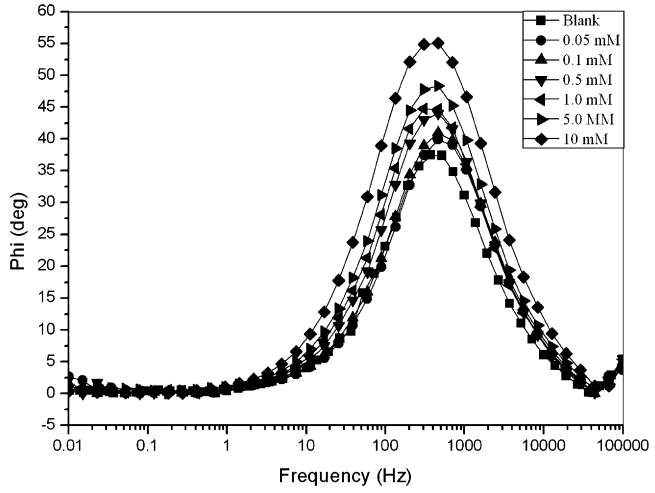

(c)

Fig. 1. Electrochemical impedance plots of mild steel in 0.5 M H_2SO_4 in the absence and presence of MTI: (a) Nyquist, (b) Bode, and (c) phase-angle plots.

the impedance is a maximum ($-Z''_{max}$) from the equation [18]

$$f(-Z''_{max}) = \frac{1}{2\pi C_{dl} R_t}. \quad (2)$$

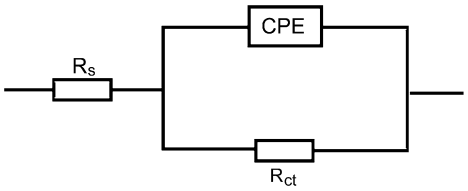

Fig. 2. The electrochemical equivalent circuit used to fit the impedance spectra.

Table 1
Electrochemical impedance parameters for mild steel in 0.5 M H_2SO_4 with methionine (MTI)

MTI conc. (mM)	R_{ct} (Ω cm^2)	n	Y_0 ($\mu\Omega^{-1}$ s^n cm^{-2})	C_{dl} (μF cm^{-2})	η%
0	8.6	0.89	221	95	–
0.05	9.3	0.91	197	84	6.7
0.1	10.1	0.90	181	77	11.6
0.5	12.7	0.91	169	74	34.6
1.0	14.7	0.91	155	83	41.4
5.0	18.4	0.91	146	64	53.0
10	29.7	0.91	124	61	71.0

The values of the electrochemical parameters derived from the Nyquist plots are given in Table 1. It is observed that introduction of MTI into the acid corrodent leads to an increase in the charge transfer resistance and a reduction of the double-layer capacitance, which become more pronounced as the MTI concentration is increased. The decrease in C_{dl} values, which normally results from a decrease in the dielectric constant and/or an increase in the double-layer thickness, is due to inhibitor adsorption onto the metal/electrolyte interface [17–20]. This implies that an increase in MTI concentration correspondingly reduces the corrosion rate of the mild steel specimen by virtue of adsorption onto the metal/electrolyte interface, thereby protecting the metal from the attack of the corrodent. The parameter n is generally accepted to be a measure of surface inhomogeneity, and its increase in the inhibited solution compared to the pure acid is connected with a decrease in heterogeneity resulting from inhibitor adsorption.

Inhibition efficiency (η%) is observed from Table 1 to increase with MTI concentration. The values were estimated by comparing the values of the charge transfer resistance in the absence (R_t) and presence of inhibitor ($R_{t(inh)}$) as follows [17–20]:

$$\eta\% = \frac{R_{t(inh)} - R_t}{R_{t(inh)}} \times 100. \quad (3)$$

Fig. 3 shows representative plots of the Tafel polarization curve for mild steel in aerated 0.5 M H_2SO_4 solutions without and with different concentrations of MTI. The introduction of MTI into the acid solution affects both the anodic and cathodic parts of the curve, while the corrosion potential (E_{corr}) is only slightly shifted. This implies that MTI functions herein as a mixed-type inhibitor. Table 2 illustrates the electrochemical parameters obtained from the polarization experiments. The results show that the corrosion current density i_{corr} decreased with increasing concentration of MTI, indicating an inhibiting effect. Also, MTI caused no pronounced change in the anodic

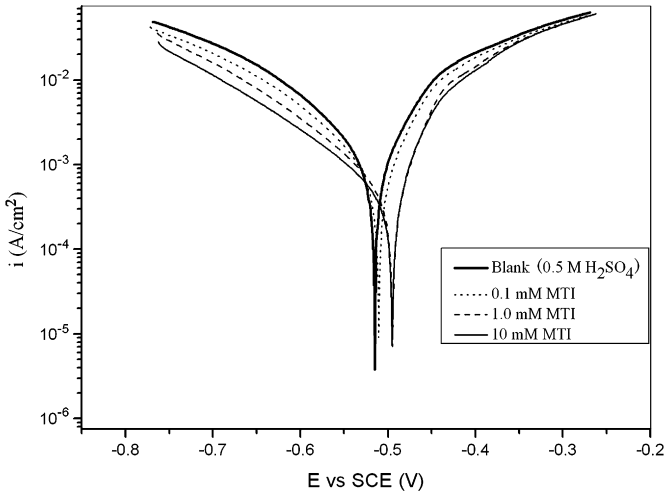

Fig. 3. Polarization curves of mild steel in 0.5 M H_2SO_4 in the absence and presence of MTI.

Table 2
Polarization data for mild steel in 0.5 M H_2SO_4 with methionine (MTI)

MTI conc. (mM)	E_{corr} (mV)	i_{corr} (μA cm^{-2})	β_c (mV dec^{-1})	β_a (mV dec^{-1})	η%
0	−514	294	215	166	–
0.05	−502	282	216	165	4.1
0.1	−508	227	201	159	22.8
0.5	−502	192	201	144	35.0
1.0	−500	166	196	141	43.5
5.0	−497	133	196	132	54.8
10	−495	87	190	112	70.4

and cathodic Tafel slopes, suggesting that the inhibitor adsorbs onto the metal surface and retards corrosion by blocking the active sites without altering the anodic and cathodic reaction mechanisms. Inhibition efficiency was calculated from the polarization data as [17–20]

$$\eta\% = \frac{i_{corr} - i_{corr(inh)}}{i_{corr}} \times 100, \tag{4}$$

where i_{corr} and $i_{corr(inh)}$ are respectively the corrosion current densities in the absence and presence of inhibitor. It is observed that the η% values obtained are in close agreement with those determined from electrochemical impedance spectroscopy measurements.

3.2. Adsorption considerations

The increase in efficiency of inhibition with concentration indicates that more MTI molecules are adsorbed on the metal surface at higher concentration, leading to greater surface coverage. The reduced effectiveness observed at low inhibitor concentrations could be related to several factors, including the relatively small molecular area of MTI, which may perhaps afford modest coverage, as well as the solubility of the adsorbed intermediate formed on the metal surface. It is generally accepted that the first step in the adsorption of an organic inhibitor on a metal surface usually involves the replacement of one or more water molecules adsorbed at the metal surface [21]:

$$Inh_{(sol)} + xH_2O_{(ads)} \rightleftharpoons Inh_{(ads)} + xH_2O_{(sol)}. \tag{5}$$

The inhibitor may then combine with freshly generated Fe^{2+} ions on the steel surface, forming metal–inhibitor complexes:

$$Fe \rightarrow Fe^{2+} + 2e, \tag{6a}$$

$$Fe^{2+} + Inh_{(ads)} \rightarrow [Fe\text{–}Inh]^{2+}_{(ads)}. \tag{6b}$$

The resulting complex could, depending on its relative solubility, either inhibit or catalyze further metal dissolution; hence the integrity depends on the environmental capacity to dilute it. Thus it is possible to suggest that at low concentrations the amount of MTI in the solution was insufficient to form a compact complex with the metal ions, so that the resulting adsorbed intermediate was readily soluble in the acidic environment. As the concentration is increased, more MTI molecules become available for complex formation, which subsequently diminishes the solubility of the surface layer, leading to improved inhibiting effect.

The mixed-inhibition mechanism suggested by the polarization data is consistent with our earlier findings [22] and those of El Azhar et al. [23] on the adsorption behavior of organic molecules containing both N and S atoms. In acid solutions, organic inhibitors may interact with the corroding metal and hence affect the corrosion reaction in more than one way, sometimes simultaneously. It is therefore often difficult to assign a single general inhibition mechanism, since the mechanism may change with experimental conditions. The adsorption mechanism for a given inhibitor depends on such factors as the nature of metal and corrosive medium, the pH, and the concentration of the inhibitor as well as the functional groups present in its molecule, since different groups are adsorbed to different extents. For instance, S-containing substances have been shown to preferentially chemisorb on the surface of iron in acidic media, whereas N-containing substances tend to favor physisorption [24]. Again, the presence of more than one functional group has been reported to often lead to changes in the electron density of a molecule, which could influence its adsorption behavior [25]. In acidic solution, MTI can be protonated at the amine group, even though the presence of S–CH_3 decreases the stability of the positive charge. The inhibitor could interact with the corroding steel surface via the protonated amino function, which can be adsorbed at cathodic sites and hinder the hydrogen evolution reaction, or via the S atom in the aliphatic chain, which may adsorb at anodic sites and retard Fe electrodissolution. The compound thus has the ability to influence both the cathodic and anodic partial reactions, giving rise to the mixed inhibition mechanism observed. Interactions giving rise to the chemisorption model based on the S atom probably start to become significant as concentration is increased, which might be responsible for the slight shift in E_{corr} toward the anodic direction, as can be discerned at high concentrations. The considerations leading to this assumption are discussed in more detail elsewhere [22]. All the same, Moretti et al. [6] observed similar phenomena, i.e., chemisorption at higher concentrations, for tryptamine, an amino acid derivative, on iron in 0.5 M H_2SO_4

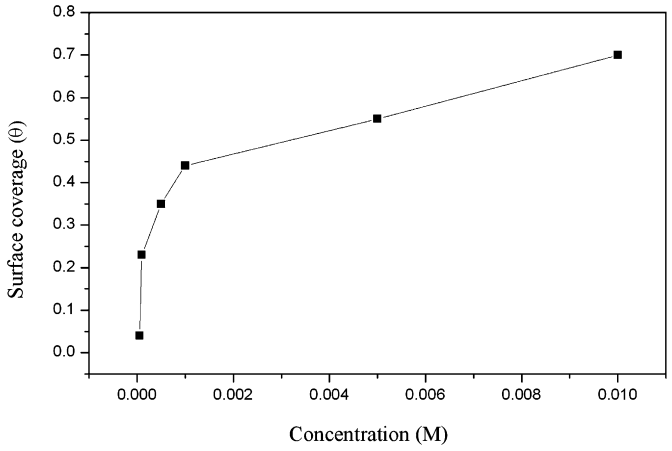

Fig. 4. Adsorption curve of MTI on mild steel in 0.5 M H_2SO_4.

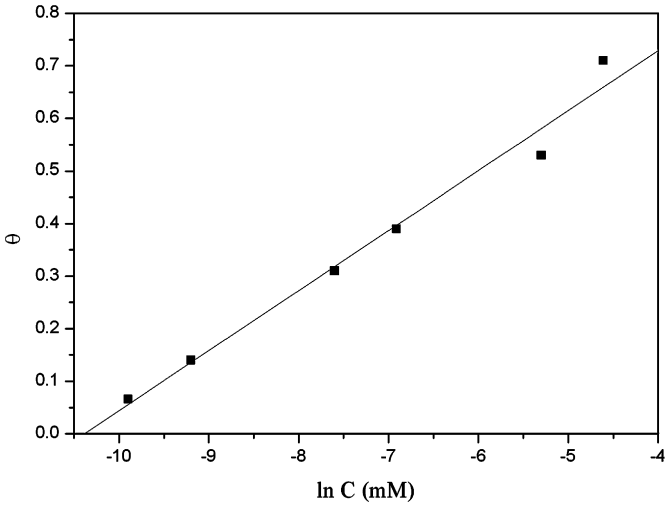

Fig. 5. Temkin isotherm for MTI adsorption on mild steel in 0.5 M H_2SO_4.

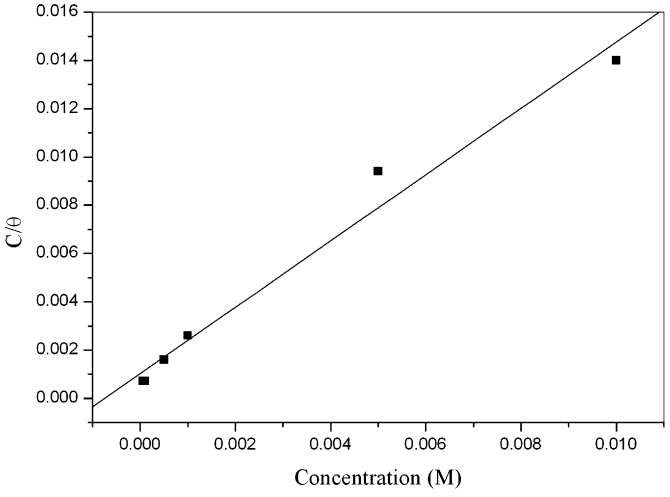

Fig. 6. Langmuir adsorption isotherm for MTI on mild steel in 0.5 M H_2SO_4.

solution. Larabi et al. [19] and Popova et al. [20] also reported comparable adsorption effects for organic inhibitors containing N and S atoms. Such behavior may also be considered in line with an earlier suggestion by Shaw [26] that a molecule may first physically adsorb, and then slowly react with the metal surface to form a chemisorbed layer.

3.3. Adsorption isotherms

Assuming a direct relationship between inhibition efficiency ($\eta\%$) and surface coverage (θ) [$\eta\% = 100 \times \theta$] for different inhibitor concentrations, data obtained from EIS measurements were adapted to determine the adsorption characteristics of MTI on mild steel in 0.5 M H_2SO_4 solution. Fig. 4 shows the adsorption curve for MTI on the steel surface, illustrating the relationship between surface coverage and concentration. The plot is characterized by an initial steeply rising part indicating the formation of a monolayer adsorbate film on the steel surface [27], and as more inhibitor molecules become adsorbed at higher concentration, the adsorption rate is reduced. To clarify the nature of adsorption, theoretical fitting to different isotherms was undertaken and the correlation coefficients (r^2) were used to determine the best fit, which was obtained with Temkin's isotherm ($r^2 = 0.990$) and the Langmuir isotherm ($r^2 = 0.989$). The Temkin isotherm characterizes the chemisorption of uncharged molecules on a heterogeneous surface, where θ is a linear function of $\ln C$ [28],

$$\theta = (1/f) \ln K_{\text{ads}} C, \tag{7}$$

f is a factor of energetic inhomogeneity in the surface, C is the adsorbate concentration, and K_{ads} is the equilibrium constant for the adsorption process, which is related to the standard free energy of adsorption (ΔG^0_{ads}) by

$$K_{\text{ads}} = \frac{1}{55.5} \exp\left(-\frac{\Delta G^0_{\text{ads}}}{RT}\right). \tag{8}$$

The linear plot of θ vs $\ln C$ as shown in Fig. 5 is in agreement with the Temkin equation. The calculated values of the adsorption parameters f, $\ln K$, and ΔG^0_{ads} are 3.85, 10.35, and -35.6 kJ mol^{-1}, respectively. The large negative value of ΔG^0_{ads} implies that the adsorption of MTI on the steel surface is allowed from thermodynamics point of view and indicates that the inhibitor is strongly adsorbed.

The Langmuir isotherm is given by [29]

$$\frac{C}{\theta} = \frac{1}{K_{\text{ads}}} + C. \tag{9}$$

The plot of C/θ vs C is shown in Fig. 6 to be linear, with slope 1.37. Though the linearity of the plot may be interpreted to suggest that the experimental data for MTI obey the Langmuir adsorption isotherm, the considerable deviation of the slope from unity shows that the isotherm cannot be strictly applied. This deviation from unity is attributable to interactions between adsorbate species on the metal surface [22,30] as well as changes in the adsorption heat with increasing surface coverage [31], factors that were not taken into consideration in derivation of the isotherm. The adsorption behavior of MTI can be more appropriately represented by a modified Langmuir equation suggested by Villamil et al. [32] as follows:

$$\frac{C}{\theta} = \frac{n}{K_{\text{ads}}} + nC. \tag{10}$$

The fit of the experimental data to the above isotherms further confirms the mixed inhibition mechanism suggested by the electrochemical measurements. In an earlier report [22], we observed that such behavior could be attributable to the possibility of multilayer physisorption on top of the chemisorbed monolayer, as suggested in [26].

3.4. Effect of KI additives

The anodic dissolution of steel in aqueous solution is known to be significantly facilitated by hydroxyl ions, which form intermediate catalytic complexes on the metal surface [33]:

$$\mathrm{Fe} + \mathrm{OH}^- \rightleftharpoons (\mathrm{FeOH})_{\mathrm{ads}} + e, \tag{11a}$$

$$(\mathrm{FeOH})_{\mathrm{ads}} \overset{\mathrm{rds}}{\rightarrow} \mathrm{FeOH}^- + e, \tag{11b}$$

$$\mathrm{FeOH}^+ + \mathrm{H}^+ \rightleftharpoons \mathrm{Fe}^{2+} + \mathrm{H_2O}. \tag{11c}$$

Halide ions, at some concentrations, may replace hydroxyl ions adsorbed on the surface of the metal, thus leading to a reduction in the catalytic effect of the hydroxyl ions [34,35],

$$\mathrm{Fe} + \mathrm{H_2O} + \mathrm{X}^- \rightleftharpoons (\mathrm{FeXOH})^-_{\mathrm{ads}} + \mathrm{H}^+ + e, \tag{12a}$$

$$(\mathrm{FeXOH})^-_{\mathrm{ads}} \overset{\mathrm{rds}}{\rightarrow} \mathrm{FeXOH} + e, \tag{12b}$$

$$\mathrm{FeXOH} + \mathrm{H}^+ \rightleftharpoons \mathrm{Fe}^{2+} + \mathrm{X}^- + \mathrm{H_2O}. \tag{12c}$$

where X represents the halide ion. This ability increases in the order $Cl^- < Br^- < I^-$ [9,22] and is initiated by the specific adsorption of the anion onto the metal surface. The greater influence of the iodide ion is often attributed to its large ionic radius, high hydrophobicity, and low electronegativity, compared to the other halide ions [22,36].

Fig. 7 illustrates the polarization curves for mild steel in 0.5 M H_2SO_4 containing different concentrations of KI. It is observed that the addition of KI reduced the rates of both the cathodic hydrogen evolution and the anodic Fe dissolution. The decrease in corrosion rate and positive shift of E_{corr} with increase in KI concentration are similar to those reported elsewhere [11]. The inhibition efficiencies displayed by the studied KI concentrations were 52.0, 50.6, 64.2, and 67.6%, respectively, for 0.5, 1.0, 2.5, and 5.0 mM KI. The values are somewhat lower than those reported in [37] for pure iron in deaerated iodine-containing 0.5 M H_2SO_4 solution. The disparity may be due to differences in the electrode materials and solution conditions. Effectiveness of inhibition depends largely on the amount of adsorbed iodide ions on active Fe sites on the electrode surface, which may be fewer in mild steel than in pure iron [12].

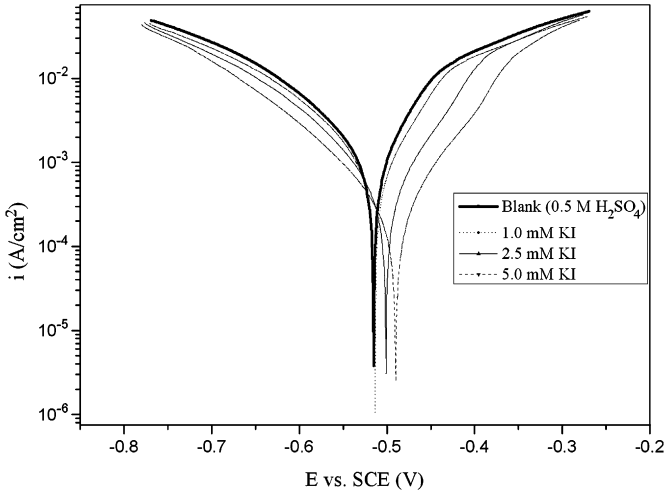

Fig. 7. Polarization curves of mild steel in 0.5 M H_2SO_4 in the absence and presence of KI.

It is generally accepted that the presence of halide ions in acidic media synergistically increases the inhibition efficiency of some organic compounds. It is thought that the halide ions are able to improve adsorption of the organic cations by forming intermediate bridges between the positively charged metal surface and the positive end of the organic inhibitor. Corrosion inhibition synergism thus results from increased surface coverage arising from ion-pair interactions between the organic cations and the anions. The influence of different concentrations of KI on the polarization behavior of mild steel in 0.5 M H_2SO_4 containing 5.0 mM MTI, corresponding to [KI]/[MTI] ratios of 0.1, 0.2, 0.5, and 1.0, respectively, is depicted in Fig. 8 and the electrochemical data listed in Table 3. The MTI–KI combinations produce pronounced effects on the anodic and cathodic currents compared to those displayed by only MTI and shift E_{corr} in the anodic direction. Also, the corrosion current density

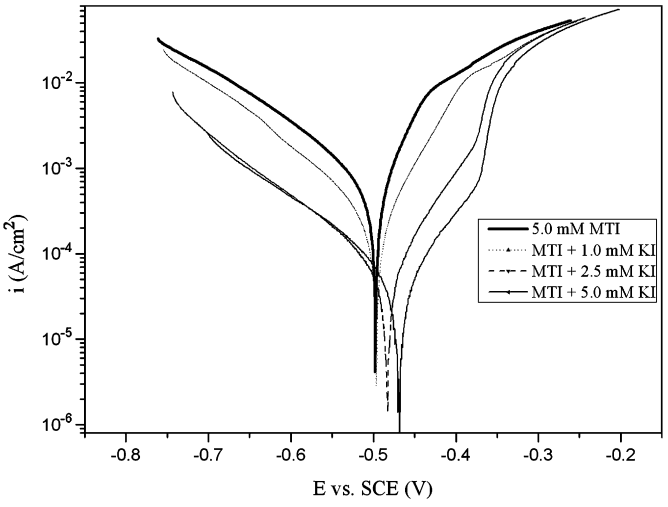

Fig. 8. Polarization curves of mild steel in 0.5 M H_2SO_4 with 5.0 mM MTI and different concentrations of KI.

Table 3
Polarization and electrochemical impedance parameters for mild steel in 0.5 M H_2SO_4 with 5.0 mM MTI and different concentrations of KI

KI conc.	Polarization method			Impedance method		
(mM)	E_{corr} (mV)	i_{corr} ($\mu A\,cm^{-2}$)	$\eta\%$	R_{ct} ($\Omega\,cm^2$)	Y_0 ($\mu\Omega^{-1}\,s^n\,cm^{-2}$)	$\eta\%$
0	−497	133	54.8	18.4	146	53.0
0.5	−492	31	89.5	33.5	119	74.2
1.0	−492	22	92.5	59.3	106	85.5
2.5	−483	6.8	97.7	243	56	96.4
5.0	−468	5.3	98.2	375	51	97.7

decreases substantially, leading to higher inhibition efficiency, up to 89.5–98.2%, compared to 54.8% obtained for MTI alone. This indicates a synergistic effect between MTI and KI.

Synergistic effects are also revealed in the impedance spectra obtained for mild steel in the presence of different concentrations of KI added to 0.5 M H_2SO_4 inhibited by 5.0 mM MTI. The results illustrated in Fig. 9 show that increasing the concentration of KI from 0.5 to 5.0 mM leads to large increases in the diameters of the semicircles in the Nyquist plot (Fig. 9a), in the impedance of the interface in the Bode plot (Fig. 9b), and in the maximum phase angle (Fig. 9c). These increases are again more substantial than those obtained for MTI alone, as shown in Fig. 1. The impedance spectra were also analyzed with the equivalent circuit in Fig. 2 and the corresponding data given in Table 3. The results show that the addition of different concentrations of KI increased the value of R_{ct} to 33.4–375 $\Omega\,cm^2$ compared to that of MTI alone, which is 18.4 $\Omega\,cm^2$.

The observed synergistic effect results from increased surface coverage arising from ion-pair interactions between I^- ions and MTI cations. Some controversy seems to exist on the actual role of the anions as regards the improved adsorption of the organic inhibitors. The ion pairs could be formed in the bulk solution and then adsorbed from the solution onto the metal surface as follows:

$$I_s^- + MT_s^+ \rightarrow (I^-\text{–}MT^+)_s, \tag{13a}$$

$$(I^-\text{–}MT^+)_s \rightarrow (I^-\text{–}MT^+)_{ads}. \tag{13b}$$

On the other hand, ion-pair formation could result from initial contact adsorption of the iodide ions on the metal surface, which leads to a recharging of the electrical double layer. The inhibitor is then drawn into the double layer by the adsorbed anions such that ion-pair formation occurs directly on the metal surface:

$$I_s^- \rightarrow I_{ads}^-, \tag{14a}$$

$$I_{ads}^- + MT_s^+ \rightarrow (I^-\text{–}MT^+)_{ads}. \tag{14b}$$

I_s^-, MT_s^+, and $(I^-\text{–}MT^+)_s$ represent the inhibitor, halide ion, and ion pair, respectively, in the bulk of the solution, while I_{ads}^-, MT_{ads}^+, and $(I^-\text{–}MT^+)_{ads}$ refer to the same species in the adsorbed state.

Wu et al. [38] proposed the first mechanism to account for the effect of iodide ions in improving the inhibition efficiency of benzotriazole during copper corrosion in sulfuric acid solution. On the other hand, results from our earlier studies [9,23,39,40], as well as those of other authors [10–14], suggest that the ion-pair interactions occur via the second mechanism. Stabilization of the adsorbed halide ions by means of electrostatic interactions with the MTI cations leads to greater surface coverage and thereby improved inhibition efficiency. Other factors could also contribute to the observed synergistic effect. Kuznetsov and Andreev [36] hinted that the chemisorption of I^- ions is capable of decreasing the hydrophilicity of metal surfaces, which is likely to promote adsorption of organic molecules. However, this effect is much less significant than the surface charge effect.

The chemisorbed MTI molecules, attached to the corroding steel surface via the S atom, might compete with I^- ions for active sites on the metal surface, leading to a lesser synergistic effect. However, our results indicate that cooperative adsorption between the specific adsorbed I^- ions and MTI cations

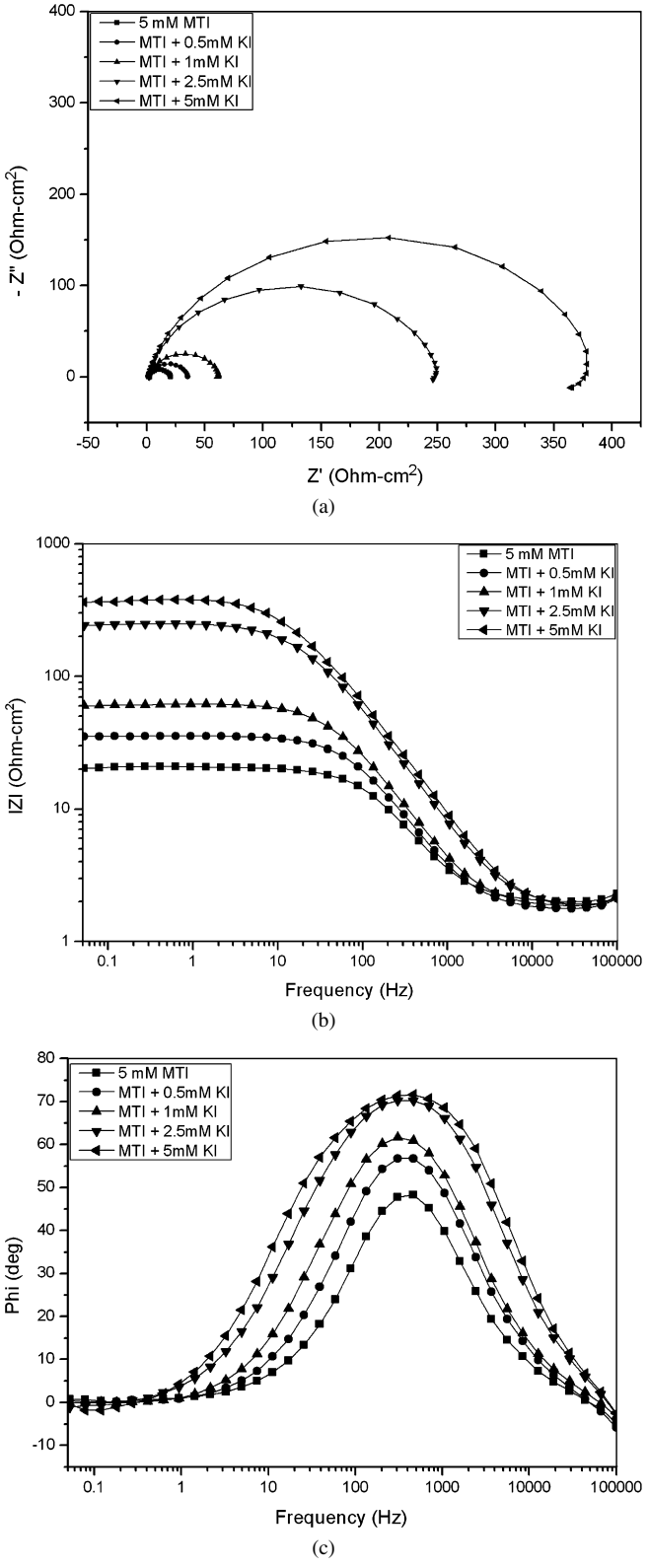

Fig. 9. Electrochemical impedance plots of mild steel in 0.5 M H_2SO_4 with 5.0 mM MTI and different concentrations of KI: (a) Nyquist, (b) Bode, and (c) phase-angle plots.

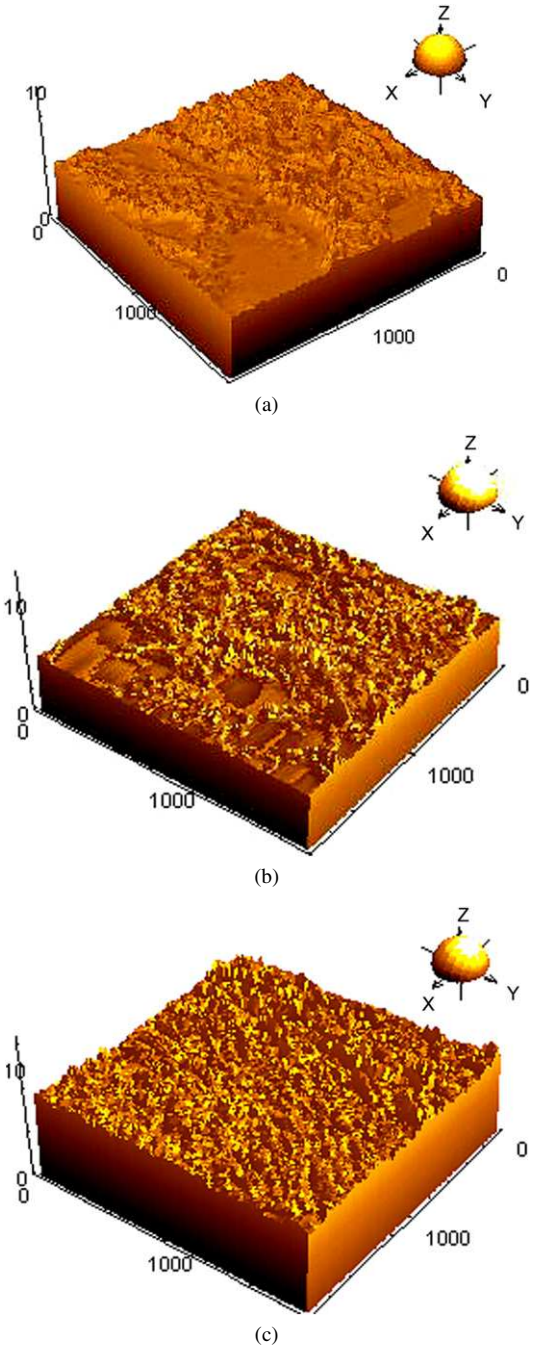

Fig. 10. AFM three-dimensional images of mild steel in 0.5 M H_2SO_4: (a) without inhibitor, (b) containing 5.0 mM MTI, and (c) containing 5.0 mM MTI + 5.0 mM KI. Scale: $X = \text{nm}$; $Y = \text{nm}$; $Z = \text{nm}$.

predominates over the competitive effect. The synergistic effect increases with KI concentration due to increased population of specific adsorbed I^- ions available for ion-pair formation with MTI cations. The highest inhibition efficiency was obtained at [KI]/[MTI] = 5/5, which is the optimum ratio of KI and MTI, and is similar to that reported by Feng et al. [12] for the synergistic effect of propargyl alcohol and KI. Excessive amounts of KI have, however, been shown by Harek and Larabi [14] to lead to occupation of the limited active sites available for inhibitor adsorption and adversely affect the inhibition efficiency.

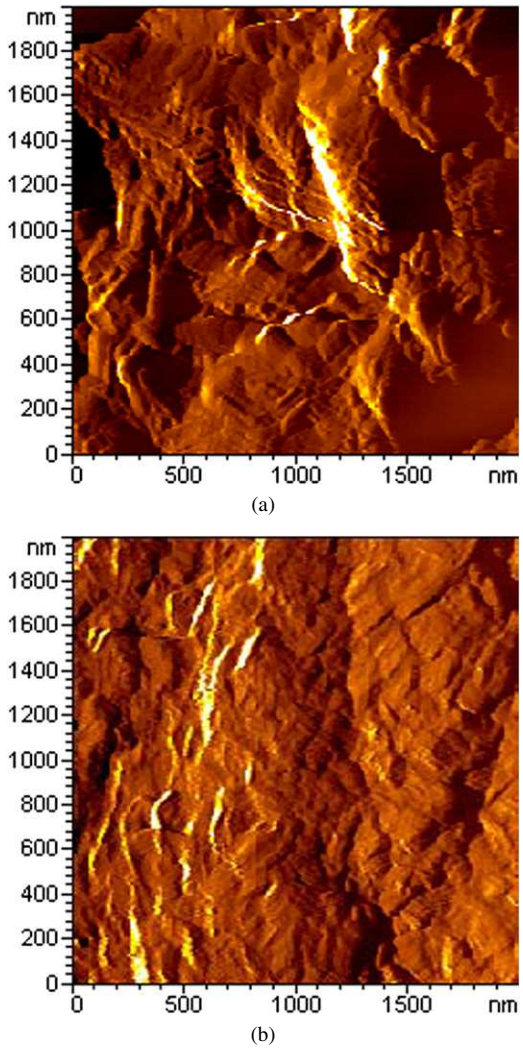

Fig. 11. AFM two-dimensional images of mild steel in 0.5 M H_2SO_4 containing: (a) 5.0 mM MTI and (b) 5.0 mM MTI + 5.0 mM KI. Scale: $X = \text{nm}$; $Y = \text{nm}$.

3.5. Atomic force microscopy (AFM) surface examination

Morphological studies of the surfaces of the mild steel specimen were followed by AFM in the range 0 to 2000 nm at room temperature after immersion in different test solutions for 3 h. Three-dimensional AFM images of mild steel in 0.5 M H_2SO_4 are shown in Fig. 10. Fig. 11 illustrates the corresponding two-dimensional images of the steel surface in the presence of additives. A rough surface is observed due to rapid corrosion of the steel specimen in the absence of inhibitor (Fig. 10a). In the presence of MTI the steel surface is less corroded and a different surface morphology is formed as well (Fig. 10b), with small spherical particles observed to cover parts of the steel surface, which corresponds to the protective formation of an inhibitor layer. The inhibitor layer formed is not very compact (Fig. 11a) and as such does not provide absolute coverage (∼0.5), with some metal surface sites still exposed to corrodent attack. A reason for this could be the short time interval available for inhibitor adsorption. In the presence of KI, however (Figs. 10c and 11b), the inhibitor layer becomes much

more compact and covers almost the entire steel surface due to synergistic interactions between iodide ions and MTI cations, resulting in the high inhibition efficiency observed in this system (∼97%).

4. Conclusions

Methionine functions as an inhibitor of mild steel corrosion in 0.5 M H_2SO_4 solution. A mixed-inhibition mechanism is proposed for the protective effect and corrosion inhibition efficiency increased with concentration. The adsorption behavior was approximated by the Temkin isotherm and a modified Langmuir isotherm. Inhibition efficiency was significantly increased by addition of small amounts of KI. The synergistic effect of KI results from increased adsorption of MTI cations by electrostatic interaction with I^- ions preadsorbed on the steel surface.

Acknowledgments

E.E. Oguzie is grateful to the Chinese Academy of Sciences (CAS) and the Academy of Sciences for the Developing World (TWAS) for the award of a CAS-TWAS Fellowship. L. Li is acknowledged for technical assistance with AFM surface analyses.

References

[1] E.E. Oguzie, Mater. Chem. Phys. 99 (2006) 441.
[2] E.E. Oguzie, Pigment. Res. Technol. 34 (2005) 321.
[3] E.E. Oguzie, K.L. Iyeh, A.I. Onuchukwu, Bull. Electrochem. 22 (2) (2006) 63.
[4] Y. Li, P. Zhao, Q. Liang, B. Hou, Appl. Surf. Sci. 252 (2005) 1245.
[5] M.S. Morad, A. El-Hagag, A. Hermas, M.S. Abdel Aal, J. Chem. Technol. Biotechnol. 77 (2002) 486.
[6] G. Moretti, F. Guidi, G. Grion, Corros. Sci. 46 (2004) 387.
[7] O. Oliveres, N.V. Likhanova, B. Gomez, J. Navarrete, M.E. Llanos-Serrano, E. Arce, J.M. Hallen, Appl. Surf. Sci. 252 (2006) 2894.
[8] D.Q. Zhang, L.X. Gao, G.D. Zhou, J. Appl. Electrochem. 33 (2003) 361.
[9] E.E. Oguzie, C. Unaegbu, C.N. Ogukwe, B.N. Okolue, A.I. Onuchukwu, Mater. Chem. Phys. 84 (2004) 363.
[10] S.M.A. Shibli, V.S. Saji, Corros. Sci. 47 (2005) 2213.
[11] G. Mu, X. Li, J. Colloid Interface Sci. 289 (2005) 184.
[12] Y. Feng, K.S. Siow, W.K. Teo, A.K. Hsieh, Corros. Sci. 41 (1999) 829.
[13] C. Jeyaprabha, S. Sathiyanarayanan, G. Venkatachari, Electrochim. Acta 51 (2006) 4080.
[14] Y. Harek, L. Larabi, Kem. Ind. 53 (2) (2004) 55.
[15] H. Ashassi-Sorkhabi, Z. Ghasemi, D. Seifzadah, Appl. Surf. Sci. 249 (2005) 408.
[16] K.F. Khaled, N. Hackerman, Electrochim. Acta 48 (2003) 2715.
[17] S.Y. Sayed, M.S. El-Deab, B.E. El-Anadouli, B.G. Ateya, J. Phys. Chem. B 107 (2003) 5575.
[18] M. Kissi, M. Bouklah, B. Hammouti, M. Benkaddour, Appl. Surf. Sci. 252 (2006) 4190.
[19] L. Larabi, Y. Harek, O. Benali, S. Ghalem, Prog. Org. Coat. 54 (2005) 256.
[20] A. Popova, E. Sokolova, S. Raicheva, M. Christov, Corros. Sci. 45 (2003) 33.
[21] J.O. Bockris, D.A.J. Swinkels, J. Electrochem. Soc. 11 (1964) 736.
[22] E.E. Oguzie, G.N. Onuoha, A.I. Onuchukwu, Mater. Chem. Phys. 89 (2004) 305.
[23] M. El Azhar, B. Mernari, M. Traisnel, F. Bentiss, M. Lagrenee, Corros. Sci. 43 (2001) 2229.
[24] A. Fragnani, G. Trabanelli, Corrosion 55 (1999) 653.
[25] N. Hackerman, E.L. Cook, J. Electrochem. Soc. 97 (1950) 2.
[26] D.J. Shaw, Introduction to Colloid and Surface Chemistry, Butterworths, London, 1966.
[27] M.A. Ameer, E. Khamis, G. Al-Senani, Adsorpt. Sci. Technol. 18 (2000) 177.
[28] M.S. Morad, A.M. Kamal El-Dean, Corros. Sci. 48 (2006) 3398.
[29] M. Lebrini, F. Bentiss, H. Vezin, M. Lagrenee, Corros. Sci. 48 (2006) 1279.
[30] C. Chakrabarty, M.M. Singh, P.N.S. Yadav, C.V. Agarwal, Trans. SAEST 18 (1983) 15.
[31] E.E. Oguzie, B.N. Okolue, E.E. Ebenso, G.N. Onuoha, A.I. Onuchukwu, Mater. Chem. Phys. 87 (2004) 394.
[32] R.F.V. Villamil, P. Corio, J.C. Rubin, S.M.L. Agostinho, J. Electroanal. Chem. 472 (1999) 112.
[33] J.O.M. Bockris, D. Drazic, R. Despic, Electrochim. Acta 4 (1961) 325.
[34] H. Bala, Electrochim. Acta 29 (1984) 119.
[35] R.J. Chin, K. Nobe, J. Electrochem. Soc. 119 (1972) 1457.
[36] Y.I. Kuznetsov, N.N. Andreev, Corrosion 96, NACE International, Houston, paper No. 214.
[37] C. Jeyaprabha, S. Sathiyanarayanan, S. Muralidharan, G. Venkatachari, J. Braz. Chem. Soc. 17 (2006) 61.
[38] Y.C. Wu, P. Zhang, H.W. Pickering, D.L. Allara, J. Electrochem. Soc. 140 (1993) 2971.
[39] E.E. Oguzie, Mater. Chem. Phys. 87 (2004) 212.
[40] E.E. Oguzie, 16th International Corrosion Congress, Beijing, China 2005, paper 17-45.